Proceedings of the 9th International Conference on Structural Dynamics, EURODYN 2014
Porto, Portugal, 30 June - 2 July 2014
A. Cunha, E. Caetano, P. Ribeiro, G. Müller (eds.)
ISSN: 2311-9020; ISBN: 978-972-752-165-4

Mechanical modeling of a vibration energy harvester with time-varying stiffness

B. Zaghari[1], M. Ghandchi Tehrani[1], E. Rustighi[1]
[1]Institute of Sound and Vibration, University of Southampton, S017 1BJ, UK.
E-mail: b.zaghari@soton.ac.uk, M.Ghandchi-Tehrani@soton.ac.uk, er@soton.ac.uk

ABSTRACT: In this paper, the problem of energy harvesting with a parametric harvester is presented. A single degree-of-freedom (SDOF) mechanical oscillator with time-varying stiffness subject to a harmonic base excitation is considered as a parametric harvester. A periodic time-varying stiffness is introduced to the harvester in order to generate parametric resonance. The performance of the harvester is analysed with and without the periodic stiffness coefficients. Relative displacement and the average harvested power are obtained both numerically and analytically. It is demonstrated that a small excitation can produce a large response when the system is parametrically excited with a frequency near to twice of its fundamental frequency. This enhancement of the displacement response results in an increase in the harvested energy. This response is higher when the base excitation frequency and the harvester fundamental frequency are equal. Also, it is possible to tune the parametric harvester to have parametric frequencies twice of the base excitation frequencies in order to increase the frequency bandwidth. The optimum parametric stiffness, parametric frequency and base excitation frequency are obtained to maximise the peak power.

KEY WORDS: Parametrically excited; Energy harvesting; Damped Mathieu equation; Base Excited.

1 INTRODUCTION

Energy harvesting is the transformation of ambient energy present in the environment into electrical energy. This energy is derived from different external sources such as solar power, thermal energy, wind energy, salinity gradient and kinetic energy. In our modern cities, vibrations are among the most widespread environmental energies. They occur in urban infrastructures such as buildings, bridges, underground structures, ships or even in the human body. The frequency of the mechanical excitation depends on different sources, for example in bridges, the frequency of excitation due to wind, ground movement, and human movement is less than 30 Hz. The mechanical energy from the harvester then converts to electrical energy. The electrical energy can be used to power wireless transducers such as those used in condition health monitoring, and as less maintenance is needed this makes them deployable on a large scale or at inaccessible locations. In recent years, energy harvesting has become a popular research topic and different vibration-based energy harvesting methods have been used [1-4], but little work has been done in exploiting parametric excitation in the context of vibration energy harvesting. Most of the harvesters are based on a vibrating mechanical structure, usually with additional seismic mass, where the driving force is applied parallel to the direction of the oscillatory displacement (see Figure 1a). In linear SDOF systems, the maximum displacement occurs at the resonance frequency. Linear harvesters harvest the most energy when the natural frequency of the harvester and environment frequency match. However, when the response frequency of the energy harvester does not match with the ambient frequency, the output power will decrease. This restricts the development and performance of linear harvesters. In order to solve the problem, different tuning and broadband method have been proposed [5].

Here parametrically excited systems are considered and compared with linear harvesters. Parametric resonance can occur in parametrically excited systems, when the parametric frequency is near twice the fundamental frequency [6-8]. This phenomenon can be used to harvest more vibration energy. In 2009, Daqaq et al. [9] investigated the process of energy harvesting via a parametrically excited cantilever beam. The cantilever beam was excited vertically, perpendicular to the direction of the oscillatory displacement. In this case, when the beam is excited at twice of its fundamental frequency, parametric resonance can be internally induced in the cantilever. This establishes an autoparametric resonance [10]. Autoparametric resonance which externally induced by parametric resonance, happens when the vibration of the primary system act as parametric excitation of the secondary system [10] . In Daqaq's study, the dynamic response of the system was explained by a lumped parameter non-linear model. The broadband characteristic of the harvester was obtained by optimising the coupling coefficient and the load resistance of the harvester. In 2011, Abdelkefi et al. [11] considered the same parametrically excited harvesting beam configuration but included higher modes and nonlinear effects of the piezoelectric patch in their analysis. In 2013, Jia and Seshia [12] presented a feasibility study on the use of parametrically excited bi-stable systems to increase harvested power. Recently, Jia et al. [13] investigated, numerically and experimentally, a parametrically excited MEMS vibration energy harvester. They explained the usability of parametric resonance over the fundamental mode, which was not limited by the system damping ratio. They also demonstrated an increase in power density and frequency bandwidth for the parametrically excited MEMS vibration energy harvester [14].

The above studies are based on autoparametric systems. In this paper a parametric harvester is introduced, which is a single degree-of-freedom (SDOF) mechanical oscillator with time-varying stiffness subject to a harmonic base excitation is introduced. In this system both parametric frequency (rate at which stiffness is harmonically varying) and base excitation frequency can change in order to achieve the maximum power and frequency bandwidth. This is an idealised study that, although does not take into account the energy spent for the generation of the parametric stiffness, can give indication of optimal condition of operation. Analytical and numerical approaches are used to simulate a SDOF harvester with time-varying stiffness. The nonlinearity of the system has not been considered here. A linear time invariant SDOF harvester, introduced by William and Yates [15], is compared with the parametric harvester. Analytical and numerical solutions for the transmissibility and the average harvested power for both systems are derived based on the Harmonic Balance Method and the time integration Runge-Kutta method. The analytical results are compared with numerical simulations. Different stability regions (different parametric stiffness and parametric frequencies) are considered to investigate the performance of the harvester in terms of the amount of the harvested energy.

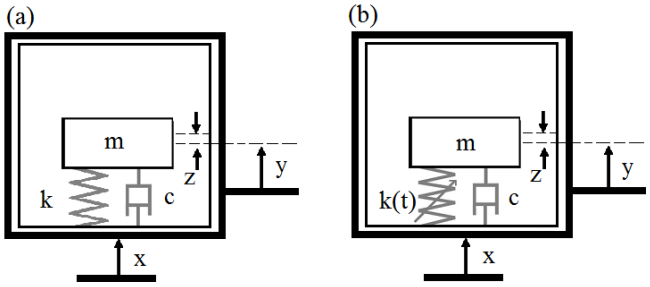

Figure 1. Single degree-of-freedom base excited system with (a) constant stiffness (b) periodic time-varying stiffness. System (a) is called the non-parametric harvester and system (b) is called the parametric harvester.

2 THEORY

A parametrically excited system is a harmonic oscillator whose parameters oscillate periodically in time. Parametrically excited systems are linear in their equation of motion with respect to displacement but their behaviour is as complex as non linear systems. The behaviour of the parametrically excited harvester and its performance is investigated. A SDOF system (parametric harvester) as shown in Figure 1b, which is subjected to a harmonic base excitation, where m is the mass, $k(t)$ is the time-varying stiffness, c is the viscous damping coefficient, y is the mass displacement and x is the base displacement. The overall damping coefficient c is associated with both dissipation and harvesting of energy, i.e the overall damping coefficient is the combination of the mechanical damping coefficient c_m and the electrical damping coefficient c_e. The electrical damping c_e represents an ideal electrical load and it is the kind of damping from which the energy can be harvested.

The governing differential equation of motion for the parametric harvester is the generic damped Mathieu equation when there is no base excitation, with respect to the relative displacement of the mass $z = y - x$

$$m\ddot{z} + c\dot{z} + k(t)z = -m\ddot{x}. \tag{1}$$

For a harmonic base excitation,

$$x = X\cos(\omega t) \tag{2}$$

where ω is the base excitation frequency. $k(t)$ is a time-varying stiffness

$$k(t) = k_c + k_p\cos(\Omega t), \tag{3}$$

where k_c is the constant stiffness and k_p is the parametric stiffness with the parametric frequency Ω. Since the system is parametrically excited, the harvester does not only respond at the fundamental frequency ω_n, but also at its combined resonances such as $\omega_n \pm \Omega$ [8].

In order to find the response of the harvester, the Harmonic Balance Method is used. Considering $z(t)$ as a Fourier series results in:

$$z(t) = A_0\cos(\omega t) + B_0\sin(\omega t) + \ldots + \sum_{m=1}^{N} A_m, B_m\cos(\omega \pm m\Omega)t + C_m, D_m\sin(\omega \pm m\Omega)t. \tag{4}$$

By substituting Equation (2) into Equation (1), the Fourier series coefficients can be found. The coefficients of sine and cosine of all harmonics are partitioned. Here, N=6 is considered to take into account the combined resonances up to $\omega_n \pm 6\Omega$. For $N = 6$, a matrix of 26×26 is produced, finding the determinant of the matrix lead to define the coefficients of the combined harmonics. Putting each coefficient back to Equation (2) gives the solution of Equation (1).

A damped Mathieu equation has an unbounded solutions (unstable regions) as well as bounded solutions (stable regions)[8]. Similarly Equation (1) has unbounded and bounded solutions for different value of parametric stiffness, parametric frequencies and damping coefficients. Different instability regions for the parametric harvester without base excitation ($x = 0$) are found here. If the solution of the homogeneous equations is asymptotically stable, then the particular solution which presents the base excitation response of the periodic system is also stable. Therefore, there is no need to find the stability curves for the base excited system since the excitation does not affect the stability curves.

For the study of the odd-occurrence stability regions, periodic solutions of period $2T$ are considered. To determine the even occurrence stability boundaries, periodic solutions of period T must be investigated. Periodic solutions of period $2T$, can be expressed as a Fourier series of the form:

$$z(t) = \sum_{m=1}^{n} A_{2m}\cos\left(\frac{2m\Omega t}{T}\right) + B_{2m}\sin\left(\frac{2m\Omega t}{T}\right). \tag{5}$$

Substituting Equation (5) into Equation (1) and setting the coefficients of $\sin\left(\frac{2m\Omega t}{T}\right)$ and $\cos\left(\frac{2m\Omega t}{T}\right)$ to zero, leads to a set of equations. The non-trivial solution of this set results in the stability threshold given as a relation between Ω and k_p.

Similarly, periodic solutions of the period T can be expressed as a Fourier series of the form:

$$z(t) = \sum_{m=1}^{N} A_{2m-1}\cos\left(\frac{(2m-1)\Omega t}{T}\right) + B_{2m-1}\sin\left(\frac{(2m-1)\Omega t}{T}\right) \quad (6)$$

Using the same procedure as for periodic solutions of period $2T$, substituting Equation (6) into Equation (1), and setting the coefficients of $\sin\left(\frac{(2m-1)\Omega t}{T}\right)$ and $\cos\left(\frac{(2m-1)\Omega t}{T}\right)$ to zero leads to another set of equations. Each of this equation represents one line in the stability curves. Finding the stability curves are important as the parametric harvester could be tuned in the stable regions.

Throughout this paper the average harvested power, P_{ave}, has been calculated both analytically and numerically in the stable regions. An average harvested power for one period can be found as:

$$P_{ave} = \frac{1}{T}\int_0^T c_e \dot{z}^2 \, dt. \quad (7)$$

3 INSTABILITY CHART FOR THE PARAMETRIC HARVESTER

Considering the method explained above, the instability chart can be found analytically. Parameters shown in Table (1) have been used throughout the work as an exemplary case to discuss more general behaviour. Parameters have been chosen to match with the work has done by Ghandchi Tehrani and Elliott [1] on energy harvesting using nonlinear damping. The instability chart for this parametric system is shown in Figure 2. In the chart, stable regions are for the system with bounded solutions, and unstable regions correspond to unbounded solutions, resulting in unstable dynamics. When the system has damping, the instability region moves upwards depending on the value of the damping ratio. This can increase the stability regions, especially at parametric frequency twice of the fundamental frequency.

Table 1. System parameters.

Parameters	Non Parametric	Parametric
Mass m (kg)	0.75×10^{-3}	0.75×10^{-3}
Stiffness k_c (Nm^{-1})	107.4	107.4
Electrical damping coefficient c_m (Nsm^{-1})	1.4×10^{-3}	85.1×10^{-3}
Harvested damping coefficient c_e (Nsm^{-1})	1.4×10^{-3}	1.4×10^{-3}
Base excitation amplitude X (m)	0.1×10^{-3}	0.1×10^{-3}
Parametric stiffness k_p (Nm^{-1})	0	64

As a result of showing the behaviour of the system, the response of the Equation (1) is plotted analytically and shown in Figure 3. The steady state response for a system when the base excitation is equal the natural frequency, $\omega = \omega_n$ and parametric excitation is twice of the base excitation frequency is considered. In order to be in the stable regions, the parametric stiffness is chosen k_p = 64 Nm^{-1} which is close to the instability curve when the instability curve starts at k_p = 64.7 Nm^{-1}. In the frequency response, it can be seen that the combination frequencies are exist in the signal. Peaks at 1 and 3 in Figure 3a show that the signal has frequencies at $\omega = \omega_n$ as well as the combined frequency $\omega_n \pm \Omega$.

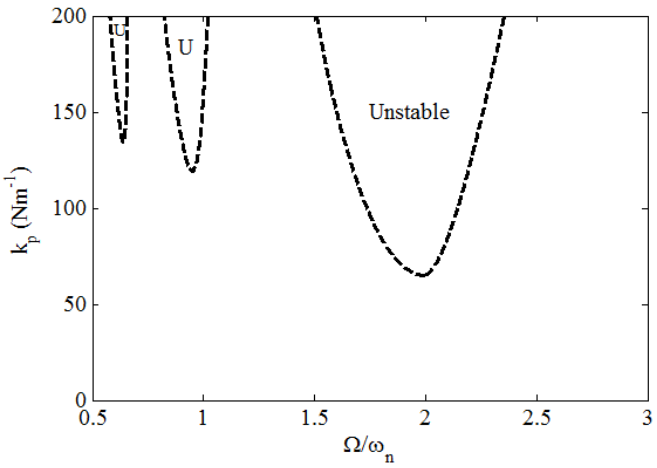

Figure 2. Analytical instability chart of the Equation (1) for a system with mass $m = 0.75\times10^{-3}$ kg and constant stiffness k_c =107.4 Nm^{-1}.

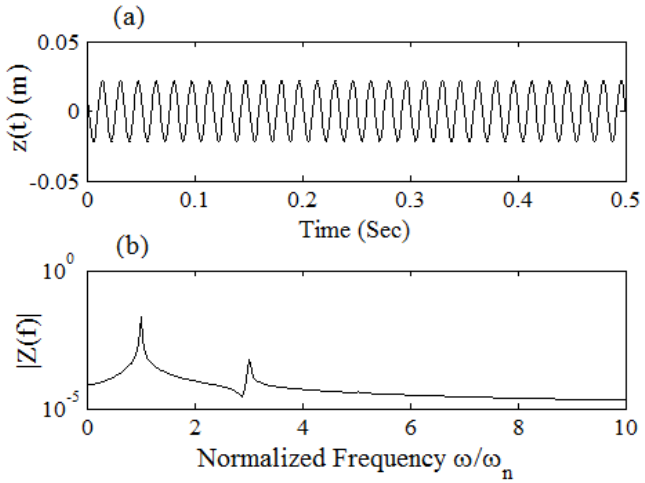

Figure 3. (a) Analytical solution and (b) the Fast Fourier Transform of the solution of Equation (1).

4 PARAMETRIC HARVESTERS VERSUS NON-PARAMETRIC HARVESTERS

In this section, the performance of the parametric harvester shown in Figure 1b is examined and compared with the non-parametric harvester of Figure 1a. The transmissibility of the harvester with parameters in Table 1 is found both analytically and numerically with the Harmonic Balance and the Runge-Kutta method. The two systems have the same mass, constant stiffness and electrical damping. If the same mechanical damping is considered the parametric harvester would present an enormous peak value at resonance. Such comparison would bring to a distorted result since in real case the stroke of the

harvester is limited by the case in which is contained. For this reason an increased mechanical damping is used for the parametric harvester so that both non-parametric and parametric systems have the same quality factors.

First, the transmissibility and average harvester power for the parametric harvester are plotted analytically for different value of parametric stiffness and parametric frequency when the base excitation is equal the natural frequency, $\omega = \omega_n$. The results for the transmissibility and average harvested power are shown in Figure 4. The instability chart found previously (section 3) is now plotted here to show the instability regions. The unstable regions are not used for harvesting power. The closer to the unstable region in which the parametric frequency is twice of the natural frequency, the greater energy can be harvested. At this frequency the stability curves start at k_p = 64.7 Nm^{-1}. For this system, the optimum parametric stiffness k_p is found close to 64Nm^{-1}. Also, it can be seen that when the parametric frequency is equal to the natural frequency the power is increased although it is not at the minimum of an instability region.

The average harvested power also is plotted numerically with ODE45, in order to show the instability regions numerically. In figure 5 the instability regions are found for the solution of Equation (1) when it was unbounded (where the solution could not go to steady sate position) and stable regions show the harvested power. The analytical instability chart has been compared with the numerical instability chart, and it is found that there is a need to increase the number of truncation order (from *N*=6 to higher) to have a more precise solution when k_p is increasing. It can be seen that as k_p is increasing there is a difference between analytical and numerical instability regions.

Now the comparison between non-parametric and parametric harvester is carried out when the parametric stiffness is equal to the optimal value found above (k_p = 64Nm^{-1}) and the parametric frequency is twice the natural frequency. The transmissibility and the average harvested power are found analytically and numerically as shown in Figure 6. The transmissibility of both systems has been intentionally considered the same by putting the different mechanical damping coefficients as shown in Table (1). The solution of Equation (1) is found analytically with Harmonic Balance Method which is explained in section 2. The numerical solution of Equation (1) is found with ODE45 and the steady state response is considered to find the transmissibility and average harvested power of the parametric harvester. The displacement of the mass $y(t)$ is found from the relative displacement of the mass $z = y - x$. The transmissibility is calculated by considering the peak to peak amplitude of the displacement for harmonic base excitation. The average harvested power for one cycle is calculated by equation (7). For the parametric harvester, two different parametric resonances are expected: $\omega = \omega_n$ and $\omega = \omega_n + \Omega$, where $\Omega = 2\omega_n$. Although, there is not a difference between the power at $\omega = \omega_n$ for the parametric harvester and non-parametric harvester, at $\omega = 3\omega_n$ the parametric has a peak which comes from its combined resonance frequencies.

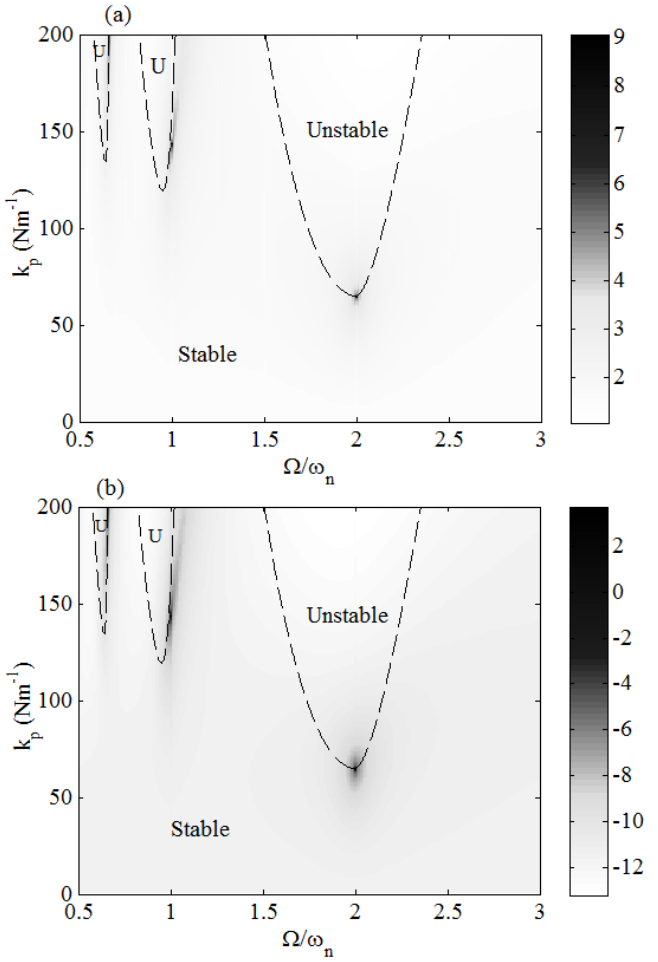

Figure 4. Analytical solution of the parametric harvester subjected to different parametric frequencies and parametric stiffness when the base excitation is equal the natural frequency, $\omega = \omega_n$: (a) natural logarithm of transmissibility and (b) natural logarithm of average harvested power.

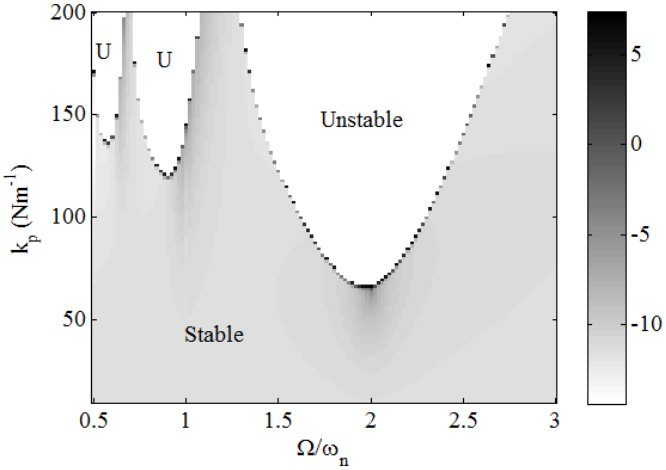

Figure 5. Numerical solution of the parametric harvester with ODE45, subjected to different parametric frequencies and parametric stiffness when the base excitation is equal the natural frequency, $\omega = \omega_n$ in order to find the natural logarithm of average harvested power.

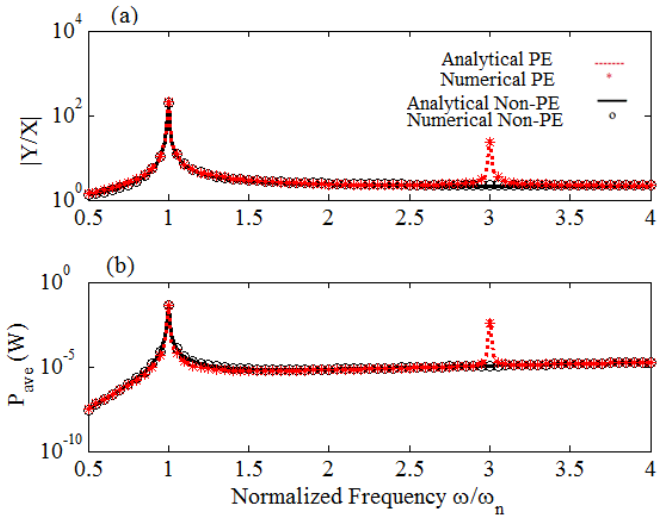

Figure 6. Analytical and numerical solution of the non-parametric and parametric harvesters with the parameters of Table 1 when $k_p = 64\text{Nm}^{-1}$ and $\Omega = 2\omega_n$: (a) transmissibility and (b) average harvested power. In parametric harvester, two different parametric resonances are expected: $\omega = \omega_n$ and $\omega = \omega_n + \Omega$, where $\Omega = 2\omega_n$.

4.1 Parametric harvester at different base excitation frequencies and parametric frequencies

Eventually, keeping the parametric stiffness equal to its optimal value of 64Nm^{-1}, the transmissibility and average harvested power are considered at different parametric frequency and base excitation frequency as shown in Figure 7. As in previous studies [11-13], when the parametric frequency is near twice of the natural frequency, greater oscillation occurs. This phenomenon can be checked for a parametric harvester subjected to a base excitation.

In Figure 7, close to the region in which the base excitation frequency is equal to the natural frequency $\omega = \omega_n$, and the parametric frequency is twice of the natural frequency, greater energy can be harvested. Also, most surprisingly, this happens when the base excitation frequency is equal to the natural frequency and parametric frequency ($\omega = \omega_n + \Omega = 3\omega_n$). Furthermore, it can be seen that in a line where both parametric and base excitation frequencies are changing (shown with Line A and B in Figure 6), the harvested power can be more broadband compared with the case in which parametric frequency is fixed and base excitation changes (Line C in Figure 6). Transmissibility and average harvested power of the parametric harvester, when the parametric frequencies are equal to $\Omega = 2\omega$ (Line A), $\Omega = \frac{2\omega}{3}$ (Line B) and $\Omega = 2\omega_n$ (Line C) are compared with the non-parametric harvester shown in Figure 9. From Figure 7, when the parametric frequency is $\Omega = 2\omega$ (Line A), the peak power at $\omega = \omega_n$ is increased, compare with the power from the parametric frequency $\Omega = 2\omega_n$ (Line C) and non-parametric harvester. Also it has more broad frequency bandwidth. However, the power does not have any peak at $\omega = 3\omega_n$.

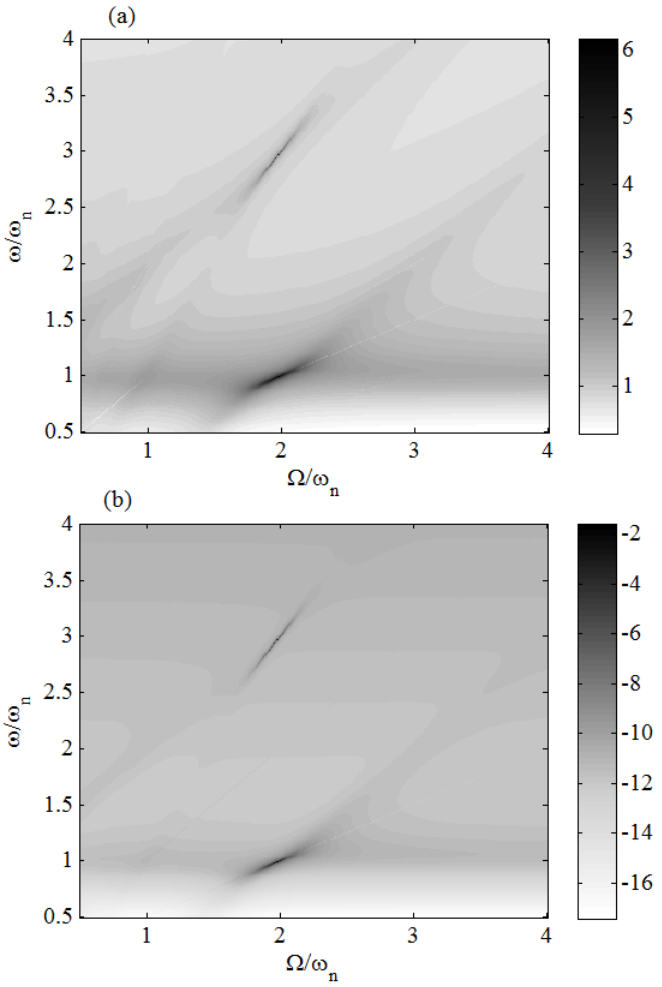

Figure 7. Parametric harvester subjected to different base excitation frequency and parametric frequency ($k_p = 64\text{Nm}^{-1}$): (a) transmissibility and (b) average harvested power. Close to the area which the base excitation frequency is equal to the natural frequency and the excitation frequency is twice of the natural frequency the higher power is harvested.

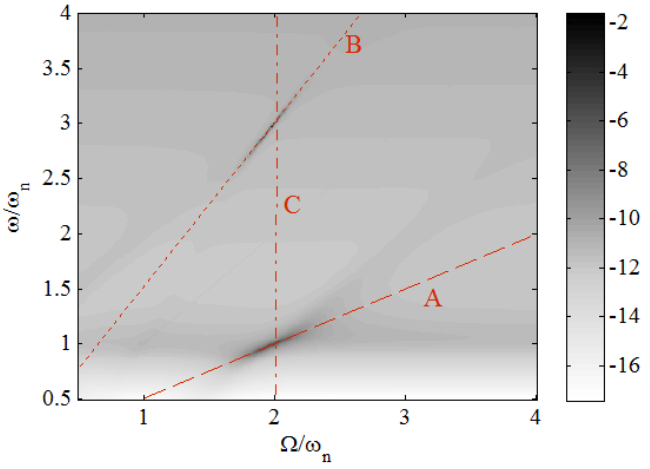

Figure 8. As Figure 7. Lines show the choice of the parametric frequency and base excitation frequency.

For the case when, the parametric frequency is $\Omega = \frac{2\omega}{3}$ (Line B), the peak power at $\omega = 3\omega_n$ is increased compared with the power with parametric frequency $\Omega = 2\omega_n$ (Line C) and non-parametric harvester. It has a more broad frequency bandwidth. However, the power does not have any peak at $\omega = \omega_n$.

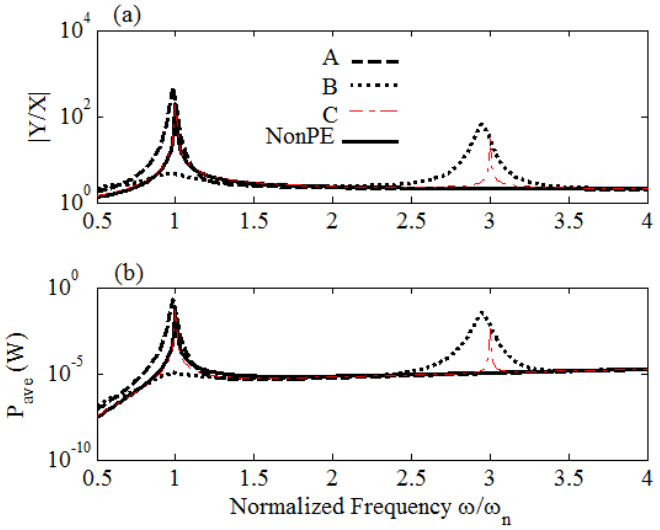

Figure 9. Analytical solution of the transmissibility (a) and average harvested power (b) when the parametric frequency is $\Omega = 2\omega$ (Line A) and $\Omega = \frac{2\omega}{3}$ (Line B), are compared with the parametric harvester transmissibility and harvested power when parametric frequency is $\Omega = 2\omega_n$ and also with the general harvester.

5 PARAMETRIC HARVESTERS VERSUS AUTOPARAMETRIC HARVESTERS

The recent work on the parametric harvesters [9-14], were based on the fact that when a cantilever beam is excited perpendicular to its oscillatory displacement, the cantilever resonates parametrically at twice of the base excitation frequency. This system has been introduced in the past as an autoparametric system. In order to harvest energy from the autoparametric excitation, the system should be tuned near twice of the natural frequency. This phenomenon can be investigated in the parametric harvester introduced here posing the base excitation equal to the natural frequency. The transmissibility and average harvested power for the parametric harvester when the parametric frequency is changing and the base excitation frequency is equal to the natural frequency of the harvester were found analytically as shown in Figure 10. Comparison of Figure 9 and Figure 10, shows that when the parametric frequency is $\Omega = 2\omega$ (Line A), the peak power is higher and also it has a larger frequency bandwidth. At lower frequencies, less than the natural frequency, the autoparametric system can harvest more power.

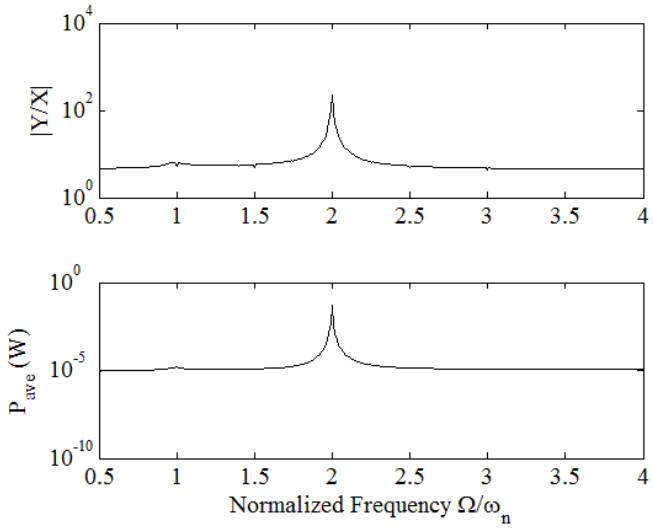

Figure 10. Analytical solution of the transmissibility (a) and average harvested power (b) when the parametric frequency is changing at different frequencies. The base excitation frequency is kept equal to the natural frequency $\omega = \omega_n$.

6 CONCLUSION

A linear SDOF harvester is compared with the parametric harvester. Analytical and numerical solutions for the transmissibility and average harvested power for both systems are derived based on the Harmonic Balance Method and the time integration Runge-Kutta method. The analytical results are compared with numerical simulations. The numerical and analytical results agree.

Stability regions for harvesters with different parametric stiffness and parametric excitation frequencies are simulated to find the optimum configuration in order to harvest more power. It was found that the parameter set closest to the start of the unstable region in which the excitation frequency is twice of the natural frequency yielded the greater energy harvest. However, in order to increase the frequency bandwidth changing the parametric frequency with the change of the base excitation were considered, as the parametric frequency can be tuned independent from the base excitation frequency. It was found that changing the parametric frequency with the change of the base excitation can broad the peak harvested power. Also these tests were compared with the fix base excitation frequency and the change of the parametric frequency (Method used in autoparametric system). The peak of the power and frequency bandwidth of the case of parametric harvester was found to be greater than autoparametric harvesters. For future work, the amount of power required to harvest energy in the proposed method will be calculated. In order to investigate furthers, experiments will be carried out to demonstrate and validate these theoretical results.

ACKNOWLEDGEMENTS

Dr Ghandchi Tehrani would like to acknowledge EPSRC for her first grant (Ref: EP/K005456/1).

REFERENCES

[1] M. Ghandchi Tehrani, S.J. Elliott, *Extending the dynamic range of an energy harvester using nonlinear damping*, Journal of Sound and Vibration, 333 (2014) 623-629.

[2] F. Di Monaco, M. Ghandchi Tehrani, S.J. Elliott, E. Bonisoli, S. Tornincasa, *Energy harvesting using semi-active control*, Journal of Sound and Vibration, 332 (2013) 6033-6043.

[3] M. Zilletti, S.J. Elliott, E. Rustighi, *Optimisation of dynamic vibration absorbers to minimise kinetic energy and maximise internal power dissipation*, Journal of Sound and Vibration, 331 (2012) 4093-4100.

[4] D. Ledezma-Ramirez, N. Ferguson, M. Brennan, *Energy dissipation using variable stiffness in a single-degree-of-freedom model*, Eurodyn2008, (2008).

[5] S.-J. Jang, E. Rustighi, M. Brennan, Y. Lee, H.-J. Jung, *Design of a 2DOF vibrational energy harvesting device,* Journal of Intelligent Material Systems and Structures, 22 (2011) 443-448.

[6] F. Dohnal, B. Mace, *Amplification of damping of a cantilever beam by parametric excitation*, (2008).

[7] F. Dohnal, W. Paradeiser, H. Ecker, *Experimental study on cancelling self-excited vibrations by parametric excitation*, in, ASME, 2006.

[8] A.H. Nayfeh, D.T. Mook, *Nonlinear oscillations*, Wiley. com, 2008.

[9] M.F. Daqaq, C. Stabler, Y. Qaroush, T. Seuaciuc-Osório, *Investigation of power harvesting via parametric excitations*, Journal of Intelligent Material Systems and Structures, 20, 545-557, 2009.

[10] A. Tondl, *Autoparametric resonance in mechanical systems,* Cambridge University Press*, 2000.*

[11] A. Abdelkefi, A. Nayfeh, M. Hajj, *Global nonlinear distributed-parameter model of parametrically excited piezoelectric energy harvesters*, Nonlinear Dynamics, 67, 1147-1160, 2012.

[12] Y. Jia, A.A. Seshia, *Directly and parametrically excited bi-stable vibration energy harvester for broadband operation,* in: Solid-State Sensors, Actuators and Microsystems, pp. 454-457, 2013.

[13] Y. Jia, J. Yan, K. Soga, A.A. Seshia, *Parametrically excited MEMS vibration energy harvesters with design approaches to overcome the initiation threshold amplitude*, Journal of Micromechanics and Microengineering, 23, 114007, 2013.

[14] Y. Jia, J. Yan, K. Soga, A.A. Seshia, *A parametrically excited vibration energy harvester*, Journal of Intelligent Material Systems and Structures, 2013.

[15] C.B. Williams, R.B. Yates, *Analysis of a micro-electric generator for micro systems*, Sensors and Actuators 52, 8-11, 1996.